New images from human visual cortex

Roger B.H. Tootell, Anders M. Dale, Martin I. Sereno and Rafael Malach

Recent developments in imaging and histology have greatly clarified our understanding of the nature and organization of human visual cortex. More than ten human cortical visual areas can now be differentiated, compared with the approximately 30 areas described in macaque monkeys. Most human areas and columns described so far appear quite similar to those in macaque but distinctive species differences also exist. Imaging studies suggest two general information-processing streams (parietal and temporal) in human visual cortex, as proposed in macaque. Several human areas are both motion- and direction-selective, and a progression of motion-processing steps can be inferred from the imaging data. Human visual areas for recognizing form are less well defined but the evidence again suggests a progression of information-processing steps and areas, beginning posterior to the human middle temporal area (or V5), and extending inferiorly then anteriorly. This is consistent with findings from macaque, and with human clinical reports.

THE FIRST evidence that cerebral cortex is composed of separate areas came from a study of part of the visual cortex[1] more than two centuries ago. Since then, research on human visual cortex has been hindered by the limited nature of non-invasive techniques. Until little over a decade ago, our understanding of the human visual cortex was confined mostly to cytoarchitectonic histology, comparatively rare brain lesions and whole-head electroencephalography[2]. Visual cortical research focused mainly on animal models, with great success. In cats, non-human primates and rodents, visual areas are now among the best-understood regions of cortex. Direct comparisons reveal a surprising degree of difference between the cortical maps in different mammalian orders[3–7].

Differences within the primate order are less striking; nevertheless, maps in prosimians, New World monkeys and Old World monkeys all differ significantly. Single-unit properties, histological features and connections also differ markedly in different primates and non-primate mammals, even when comparisons are restricted to areas considered to be homologous. The question of homology is particularly important with regard to human visual cortex because it is becoming increasingly possible to resolve human cortical areas, although single units and connections cannot yet be determined routinely. Since cortical-area maps remain constant between humans and other mammals, it can be inferred (but has not yet been proved) that single-unit properties and connections are also similar among these species.

The usual justification for studying visual cortex in macaques is their similarity to humans; excepting apes, humans are most closely related to Old World monkeys such as macaques (*Macaca*). Macaque and human vision is comparable psychophysically, except for a slight difference in long-wavelength photopigment. The anatomies of macaque and human visual systems also appear grossly similar. For example, human and macaque area V1 (also known as area 17, primary visual cortex or striate cortex) are similar with respect to the laminar and cytoarchitectonic organization[8] as well as the cytochrome oxidase architecture[9–11]. Ocular dominance columns have also been demonstrated anatomically in human V1 (Refs 9,11,12); this is especially telling because ocular dominance columns are either subtle or absent in V1 of some New World monkeys[13]. Human homologs of monkey areas V2 and the middle temporal area (MT) (or V5) are reasonably well accepted[7].

Despite these broadly defined similarities, distinct species differences begin to become apparent even in area V2. The orderly arrangement of cytochrome oxidase 'stripes' into parallel 'thin' and 'thick' stripes, so obvious in monkeys (see, for example, Ref. 14), has evolved into a disorderly jumble of patches in human V2 (Ref. 10; see also Fig. 1). It is not clear how (or if) the irregular cytochrome oxidase patches in human V2 relate to the strikingly parallel cytochrome oxidase stripes in macaque V2. On the other hand, myelin[10] and CAT-301 (Ref. 15) staining have shown orderly human V2 'stripes' consistent with an expanded version of the monkey V2 stripes.

By generalizing from macaque cortical maps, several contemporary lesion studies have reported far-reaching insights from rare clinical cases in humans. Horton and Hoyt[16] related the topography of 'quadratic' (quarter-field) visual-field deficits to the location of cortical lesions producing them, implying a human homolog of macaque cortical area V3 and suggesting its location. Using a stain that revealed long-term axonal degeneration, Clarke and Miklossy[17] were able to map the topographical pattern of callosal degeneration in one patient. This topography was then used to infer the boundaries of several visual cortical areas corresponding to vertical meridian representations, since these are known to be innervated preferentially by callosal connections. Another significant lesion study is that of Zihl *et al.*[18] who described a patient with selective deficits in the perception of visual motion due to bilateral cortical damage, including (apparently) lesions in human area MT (V5).

Roger B.H. Tootell and Anders M. Dale are at the Nuclear Magnetic Resonance Center, Massachusetts General Hospital, 149 13th St, Charlestown, MA 02129, USA. Martin I. Sereno is at the Dept of Cognitive Science, University of California at San Diego, San Diego, CA 92093-0515, USA. Rafael Malach is at the Dept of Neurobiology, Weizmann Institute for Science, Rehovot 76100, Israel.
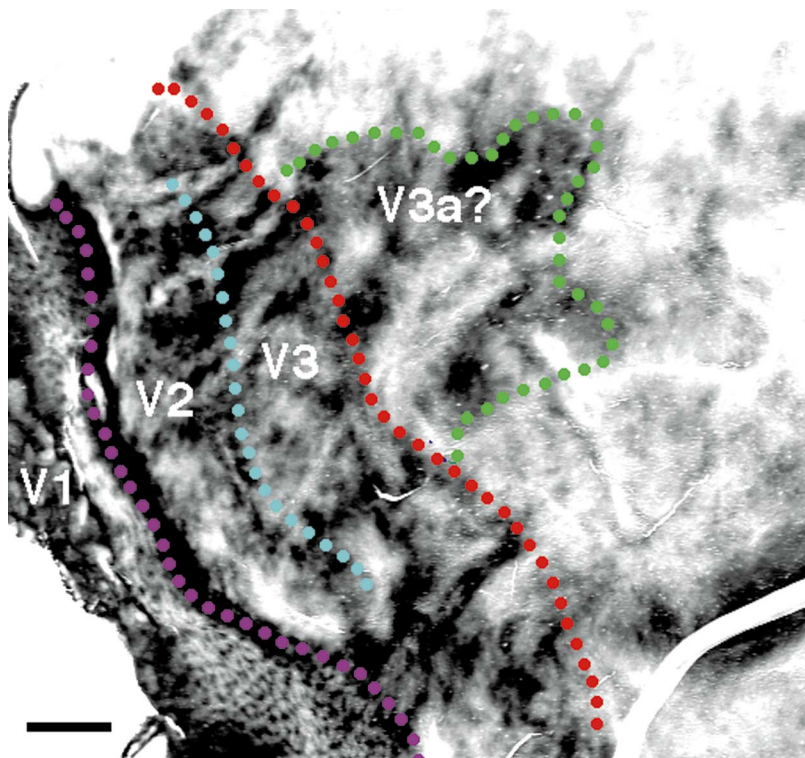
Fig. 1. *Topographical variations in cytochrome oxidase staining in flattened human visual cortex. The figure shows an image from very wide microtome sections (60 μm thick) centered on layers 3 and 4 from flattened visual cortex, after staining for cytochrome oxidase. The 'blobs' in human area V1 are clearly visible and are similar to (although larger than) those in non-human primates. Immediately surrounding this region is a belt (1.5–3 cm wide) of irregular dark patches. In this example, some of the patches are aligned in stripes orientated perpendicular to the border between areas V1 and V2, as in several species of monkey. However, the human topography is typically more patchy and less stripe-like. Human area V2 presumably occupies at least the region adjacent to the border between V1 and V2. Additional borders drawn on the figure are hypothetical, based on retinotopic measurements made by functional magnetic resonance imaging (fMRI) and subtle distinctions in the cytochrome oxidase topography. The anterior portion of the belt may be co-extensive with V3. Even further anterior, there is a pronounced (approximately 3 cm) extension of the patchy cytochrome oxidase staining (previously named 'PX'; see Ref. 10) that might include, or coincide with, human area V3A. Scale bar, 5 mm.*

So far, topographical dimensions in human visual cortex have been found to be approximately double the size of the corresponding features in macaque. This was based on the overall length and width of apparently corresponding areas such as V1, MT (V5) and V2, as well as the size of columnar systems within a given area [for example, ocular dominance columns in V1, blobs in V1, cytochrome oxidase patches in MT (V5) and myelin-based stripes in V2 (reviewed in Ref. 10)]. However, this size relationship is only a rough generality: some human areas show a greater increase in size while some show less. Such disproportionate increases and decreases might reflect the relative importance or function of corresponding areas, with respect to those areas or columns that can be assumed to be homologous (see below); this kind of rationale led to the claim that the pulvinar and frontal lobes are 'more important' in humans than in macaques because of their more-than-proportionate expansion in the human brain.

Functional imaging, topography and retinotopy

Positron emission tomography (PET) techniques were the first used to form images of the local metabolic activity of human visual cortex. Fox *et al.*[19,20] suc-

cessfully resolved three foci of activity in the calcarine fissure (presumably mainly in V1) produced by visual stimuli at correspondingly varied eccentricities. The location of these foci was generally consistent with the retinotopic information available at the time. This 'bottom-up', sensory-based PET approach achieved sustained momentum with the studies of Zeki, Frackowiak and co-workers, who were the first to demonstrate and localize human area MT (V5) (Refs 21–23) and who have since presented evidence for several other areas (see below). Other PET studies of the visual system have focused on higher-order, 'top-down' variables such as attention to different visual dimensions (see, for example, Ref. 24) and activity during language tasks[25].

This section discusses results derived from functional magnetic resonance imaging (fMRI) of intrinsic signals, a technique introduced only a few years ago[26–29]. Like PET, fMRI reflects the local changes in blood flow or oxygenation, or both (depending on several technical variables) that occur very near the neurons activated by a given experimental paradigm. The metabolic basis of the fMRI signal is not yet as thoroughly understood as that underlying the PET signals, although progress in this area of research is being made. On the other hand, fMRI signals have better spatial and temporal resolution than PET techniques and permit unlimited scanning without risks from radioactive toxicity. Therefore, certain types of functional imaging studies that were not feasible previously can now be performed. For example, functional cortical columns have been reported in fMRI experiments using high field strength and sub-millimeter (0.3–0.6 mm^2) voxels[30].

In other fMRI studies, it has been possible to visualize cortical activity in response to many types of visual stimuli given to one subject. Maps of the resultant variations in the location of visual activity can then be visualized and analysed in an 'unfolded', or 'flattened', cortical surface format. Maps of such activity-based visual 'areas' can then be compared directly with the topography of cortical visual areas defined in other subjects and with maps from other species. A map of the activity-based human areas V1, V2, V3, ventral posterior (VP), V3A, ventral V4 (V4v), lateral occipital (LO), MT (V5), posterior division of dorsal medial superior temporal area (pMSTd), lateral superior parietal occipital (LSPO) and superior parietal occipital (SPO) compared with a map of visual areas in the macaque monkey, derived from other techniques, is shown in Fig. 2. After borders of these areas have been defined using a standard set of 'diagnostic' stimuli (described in Fig. 2), the activity in each defined human area can then be tested in response to 'higher-order' visual stimuli.

The detailed retinotopy in the first defined human areas V1, V2, V3, VP and V3A (Refs 32,33,35–38) is so similar to that of macaque that these areas can reasonably be considered to be homologous (see Fig. 2 and below). Based on functional, histological and topographical similarities, 'MT (V5)' in humans is also probably homologous to macaque MT (V5) (Refs 7,10,36). Based on topographical and functional properties, human 'pMSTd' is probably homologous to the dorsal division of area MST (MSTd) in macaques (see below) but there is less evidence on this point. Evidence giving grounds for homology becomes even more sparse

in areas near the parietal–occipital juncture, in both humans and macaques. However, based on topographical and functional characteristics, human areas SPO and LSPO might be related evolutionarily to macaque ventral intraparietal (VIP) and lateral intraparietal (LIP), respectively. Areas LO and V4v are less certainly related to specific macaque areas (see below). Other functionally distinct areas clearly exist but they are not yet well enough explored to commit to a diagram.

Topographically, most of these human areas are about twice as long and twice as wide as their same-named counterparts in macaque. However, the width of human V3 and VP is disproportionately expanded by a factor much greater than that (approximately ten rather than two). This has interesting ramifications with regard to the cortical magnification factor in these regions: a pronounced radial anisotropy is present in the cortical magnification factor in macaque areas V3 and VP but is absent in human V3 and VP. The topographical distance from MT (V5) to the foveal areas V2, V3 and VP is also disproportionately expanded in humans, relative to macaque. This relatively 'expanded' region in humans might be involved in form processing (see Fig. 2 and below).

As human (and monkey) maps of visual cortex become more accurate, comparisons between them should become more illuminating. However, our understanding of human cortical retinotopy and of associated imaging techniques is already sufficient to show apparent retinotopic 'isomorphism' between visual stimuli and resultant brain activity (Fig. 3), similar to evidence of this kind of isomorphism obtained previously from animal models.

Cortical unfolding

In experimental animals, it has become commonplace to display and analyse visual cortical maps after 'unfolding' or 'flattening' the gray matter[14,34,41–43]. The rationale behind this practice is that the cortical gray matter (where essentially all neurons are located) is intrinsically a sheet several millimeters thick, which, *in vivo*, is folded for biological convenience – presumably to shorten the intracortical connections and enabling it to fit its considerable surface area inside the skull. Many fundamental mapping features (such as cortical area boundaries, columns and interlaminar axonal projections) are mapped in parallel with the cortical surface and layers. The cortical 'unfolding' procedure simply rearranges these topographical features so that they are all contained within the single plane available on a printed page or video screen. Cortical flattening approaches are now being used in human visual cortex research as well (Refs 10,33,38,44; see Figs 1–3). Although the human gray matter is folded tortuously *in vivo*, unfolding procedures do not necessarily entail any distortion. With a single longitudinal cut, a cylinder or cone can be unfolded without any distortion at all, although a sphere will be distorted by unfolding. The relevant question is whether the human cortex (or portions thereof) is more like a cylinder, a cone or a sphere.

Measurements from optimally flattened human and monkey brains yield values for residual distortion (angular and areal) of about 15% (Refs 33,34,43). However, such distortion occurs only in the displays of computationally flattened images; quantitative topographical measurements can be entirely corrected for the (known) flattening distortion[33].
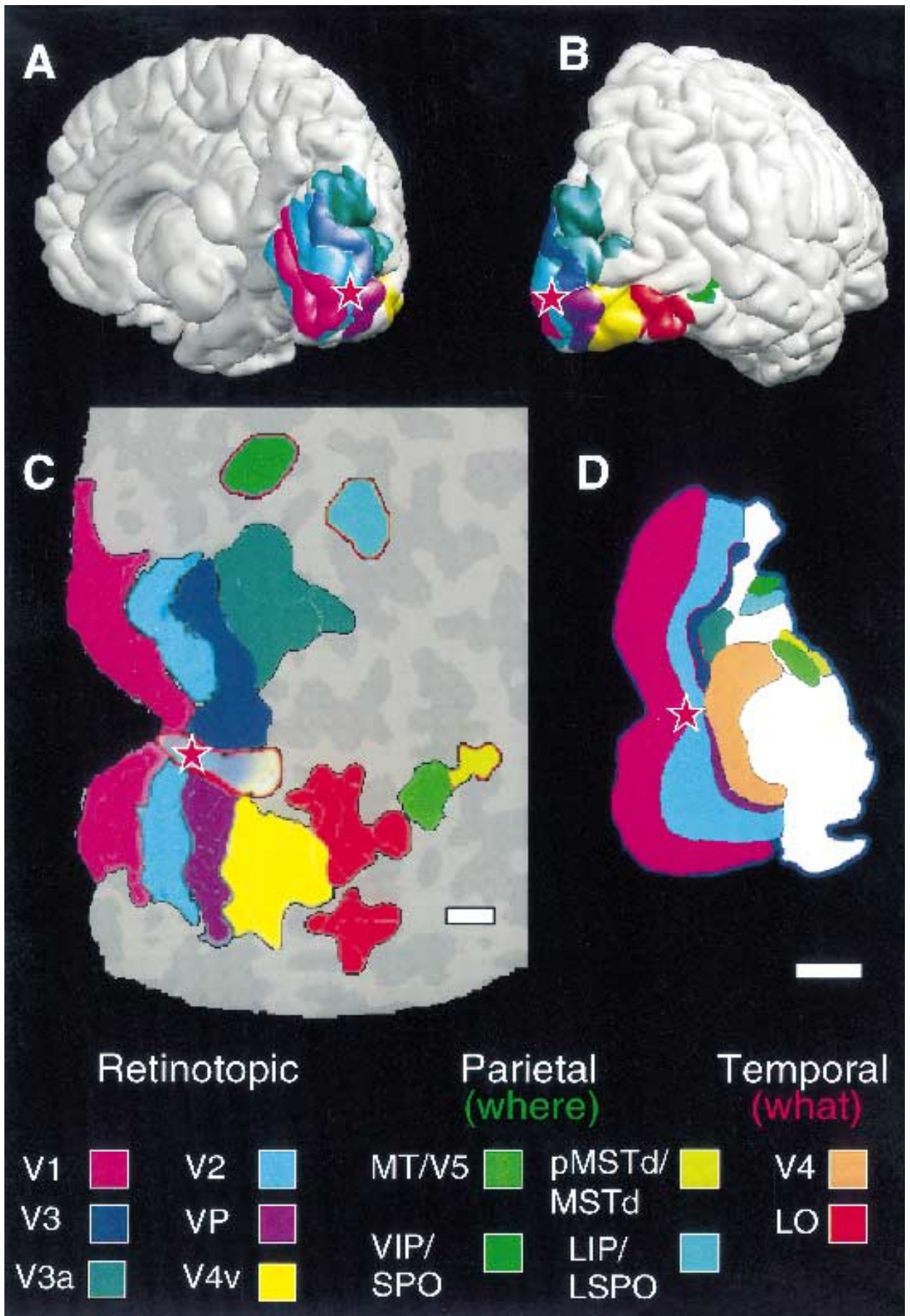
Parietal and temporal streams

In macaque visual cortex, two general information-processing 'streams' of areas have been proposed and widely discussed: a 'parietal' (or 'dorsal', or 'where') stream, processing certain aspects of visual motion, eye movements and spatial organization; and a 'temporal' (or 'ventral', or 'what') pathway, specialized for color and form recognition[45–50]. It has been suggested that additional anatomical and physiological compartments (such as magnocellular and parvocellular 'streams' in the lateral geniculate nucleus, cytochrome oxidase 'blobs' and 'interblobs' in V1, and V2 'stripe' architectures) extend the parietal and temporal streams at lower levels of the visual network but these hypothetical links have been controversial (see, for example, Refs 51,52). Unfortunately, very little is known about human intracortical connections (see below) and so there is no certainty that 'parietal' and 'temporal' streams exist anatomically in human visual cortex. Although functional imaging and evolutionary links suggest that information-processing streams related to those in macaques do exist in human visual cortex[53], other evidence[54] is inconsistent with this assumption. We do not attempt to resolve this important issue here; the contemporary view of such 'streams' is invoked only as a convenient heuristic hypothesis to discuss findings relevant to this article.

Parietal stream

It is impossible to specify the exact boundaries of the parietal and temporal streams in either human or non-human primates. However, a human parietal stream would presumably include at least areas MT (V5), MST and intraparietal areas (such as VIP and LIP), assuming homologs to these areas in macaques exist in humans; similarly, a human temporal stream would presumably include homologs of areas V4 and various inferotemporal cortical areas.

Area MT (V5) in monkeys is anatomically and physiologically quite distinctive, and has been studied extensively. Furthermore, an area homologous to MT (V5) appears to exist in all non-human primates tested, including Old World monkeys, New World monkeys and several groups of prosimians. Thus, the recent discovery and description of an MT (V5) homolog in humans was of great interest. Several histological studies (foreshown in 1920 by Flechsig[55]) reported areas of increased myelination[4,10,17], cytochrome oxidase activity[10,56] and staining by the monoclonal antibody CAT-301 (Refs 10,57) in areas of the human visual cortex that generally match the expected location, size and histological features of macaque MT (V5). The study using CAT-301 is particularly persuasive because the antibody binds to a cell-surface epitope found prominently in cells along several stages of the macaque 'magnocellular' pathway, with a distinctive laminar profile in macaque MT (V5) (Ref. 56). However, the exact location of these histological features is still uncertain in humans[4,10]. Ideally, the anatomical and functional (see below) evidence for area MT (V5) should be confirmed using fMRI in the same human individuals[58], but so far this has not been done.

It has proved easier to reveal an apparent human area MT (V5) functionally in PET and fMRI experiments[21–23,36,59–61], by comparing neuronal activation

Retinotopic

V1	V2	
V3	VP	
V3a	V4v	

Parietal (where)

MT/V5   pMSTd/MSTd

VIP/SPO   LIP/LSPO

Temporal (what)

V4

LO

produced by moving as opposed to stationary stimuli. Based on results from non-human primates, roughly half of the cells in MT (V5) should respond more in response to stimuli moving in a given local direction compared with control stimuli that are stationary and non-flickering.

As in non-human primates, this 'functional' MT (V5) area lies several centimeters anterior to the

Fig. 2. (left) *Location and topography of presumptive visual areas in human and macaque cortex.* **(A and B)** *One representative cortical hemisphere of human brain in the normal (folded) state, based on high-resolution 'anatomical' magnetic resonance images. Visual areas have been rendered in pseudocolor on to the surface, based on data from functional magnetic resonance imaging (fMRI) as described below.* **(C)** *The same anatomical and functional data depicted in 'flattened' cortical format. Additional areas (bounded by red borders) are based on data from other subjects and were added for completion. Based on quantitative differences in cortical curvature, the locations of gyri and sulci in the folded brain depicted in A and B are represented in light and dark gray, respectively, in the flattened representation in C. For comparison,* **(D)** *shows the corresponding flat map from macaque monkey, based on previously published data[31]. Both flattened maps are taken from the right hemisphere, which was artificially split along the length of the calcarine fissure (approximately the horizontal meridian representation in V1).*

Borders of human visual areas are presumptive. However, each cortical visual area in A, B and C has been reliably produced in approximately the same cortical location (with similar topographical relationships to surrounding areas, likewise defined) in several scan sessions in at least four subjects (usually many more), in response to the same visual stimulus or set of stimuli. Names for human visual areas have been adopted from apparently corresponding areas in macaque when there is both topographical and functional evidence of homology [for example, V1, V2, V3, ventral posterior (VP), V3A and middle temporal area (MT, or V5)]; this is qualified when evidence for homology is encouraging but not definite (for example, in the case of the posterior division of dorsal medial superior temporal area (pMSTd). Otherwise, new names have been invented [for example, lateral occipital (LO), SPO, LSPO]. Presumptive corresponding areas in the two primates are assigned the same color on the map. The foveal representation is a shared strip connecting most of the retinotopic areas and is centered roughly at the star. Based on fMRI data and inferences from the connectional hierarchy in macaques[31], the human areas are grouped into three broad categories: retinotopic (blues and purples); parietal (greens); and temporal (yellow to red) – obviously, such categories are heuristic and tentative.

Subjects were scanned in a 1.5 T magnetic resonance imager, retrofitted with echo-planar imaging. In each 8 min 32 s scan, 2048 images were collected [repetition time (TR) = 4 s] in multi-slice mode (16 slices; 4 mm thick) at 3 × 3 mm resolution, using a bilateral surface coil (covering occipital and posterior temporal and parietal lobes) and an asymmetric spin-echo sequence [echo time (TE) = 70 ms; offset = 25 ms]. Visual stimuli were presented to subjects within the magnet, with an extensive field of view.

Phase-encoded, retinotopically varying stimuli (thinner versions of those described in previous studies[32,33]) were used to distinguish polar angle and eccentricity axes in retinotopically organized areas. This information was combined to derive the visual field sign polarity[33], which reverses at area boundaries. The boundaries of areas V1, V2, V3, VP, V3A and ventral V4 (V4v), mapped in the same individual, were derived in this way.

The motion-responsive areas MT (V5), MSTd and V3A were selectively activated (in the same subject) by a pattern of moving concentric rings. A set of black-and-white images of objects or faces, compared with scrambled versions of the same objects or faces, were used to activate area LO selectively, again in the same subject. Some variability was observed in the location of object-selective activity across individuals.

Area LSPO responds selectively during saccade tracking, but not fixation, in near-total darkness. Area SPO is activated by the coherent motion of random, low-density dots, compared with random motion of the same set of dots, with otherwise identical motion parameters. In some subjects, area MT (V5) can be reliably and selectively activated by the motion coherence test and by tests for greater interhemispheric activation.

The topography of human cortical areas is generally similar to that in macaques, except for an overall expansion; however, there are some noteworthy differences. (1) Human maps contain a posterior anterior retinotopic area (V4v) as well as a non-retinotopic, form-related area (LO) between MT (V5) and VP, but there is no clear area border corresponding to the border between V4v and LO in current macaque maps. (2) There is proportionately more area between MT (V5) and foveal V3 and VP in human compared with macaque maps. (3) Human V3 and VP are proportionately several times wider than macaque V3 and VP. The assignment of separate names ('V3' compared with 'VP') to mirror-symmetrical, quarter-field representations (otherwise known as superior and inferior arms of V3) is based entirely on macaque data; functional differences have not yet been reported between these two areas.

In C, linear and angular distortion due to flattening is minimized and averages approximately 15% overall[33]; the corresponding distortion in D is presumably similar[34]. Scale bars, 1 cm.

---

retinotopic areas (such as V3 and VP) in the flattened maps (see Fig. 2). However, human MT (V5) is located somewhat more inferiorly in humans than it is in monkeys; technically, human MT (V5) is closer to the temporal lobe than to the parietal lobe. It also usually lies in the ascending limb of the inferior temporal sulcus[23], which is quite significantly posterior to the superior temporal sulcus and adjacent gyrus [where MT (V5) lies in all other known primates]. The more posterior location of human MT (V5) is consistent with the locations of other human visual areas such as V1, V2 and V3, which have also 'migrated' posteriorly. It is as if the whole map of human visual cortical areas has been 'pulled' as a sheet around the occipital pole, deeper into the medial bank.

Despite these localization discrepancies, presumptive human MT (V5) functions like macaque MT (V5) in many respects. Results from fMRI studies suggest that (as in the macaque area) human MT (V5) neurons are direction-selective as well as motion-selective[61], they have very high contrast-sensitivity[36], and they respond less to moving, color-varying stimuli when components of that stimulus are isoluminant[36]; human MT (V5) responds robustly even to illusory motion (Refs 61,62; see Fig. 4). Encouragingly from a clinical point of view, Eden *et al.*[63] showed that activation of area MT (V5) does not occur or is drastically decreased in a select population of dyslexics.

Although early research of the parietal stream in humans focused on human area MT (V5), other motion-selective areas in human visual cortex are now receiving increased attention. Several studies have noted motion-selective activity located superior and posterior to the MT (V5) focus. From its general location, a number of PET studies have suggested[23,59,64,65] that this area in humans might correspond to area V3 of macaques, in which approximately half the cells are motion- and direction-selective[66]. However, direct comparisons of both the retinotopy and motion selectivity in within-subject fMRI tests in humans and macaques (Ref. 36; R.B.H. Tootell, A.M. Dale, J.D. Mendok Lui, J.B. Reppas and M.I. Sereno, unpublished observations) reveal that the motion-selective area corresponds to human V3A rather than V3. Indeed, human V3 is less responsive to motion stimuli than any other cortical visual area measured (that is, areas V1, V2, V3, VP, V3A and MT). This is surprising because more motion-selective cells have been reported in macaque V3 than in V3A (Refs 66,67). Despite uncertainties about comparing macaque single-unit recordings with human fMRI, these results suggest a striking species difference in the nature of visual motion processing.

In macaques and other monkeys, area MT (V5) is bordered by several small satellite areas that share prominent interconnections and refine the motion-selective
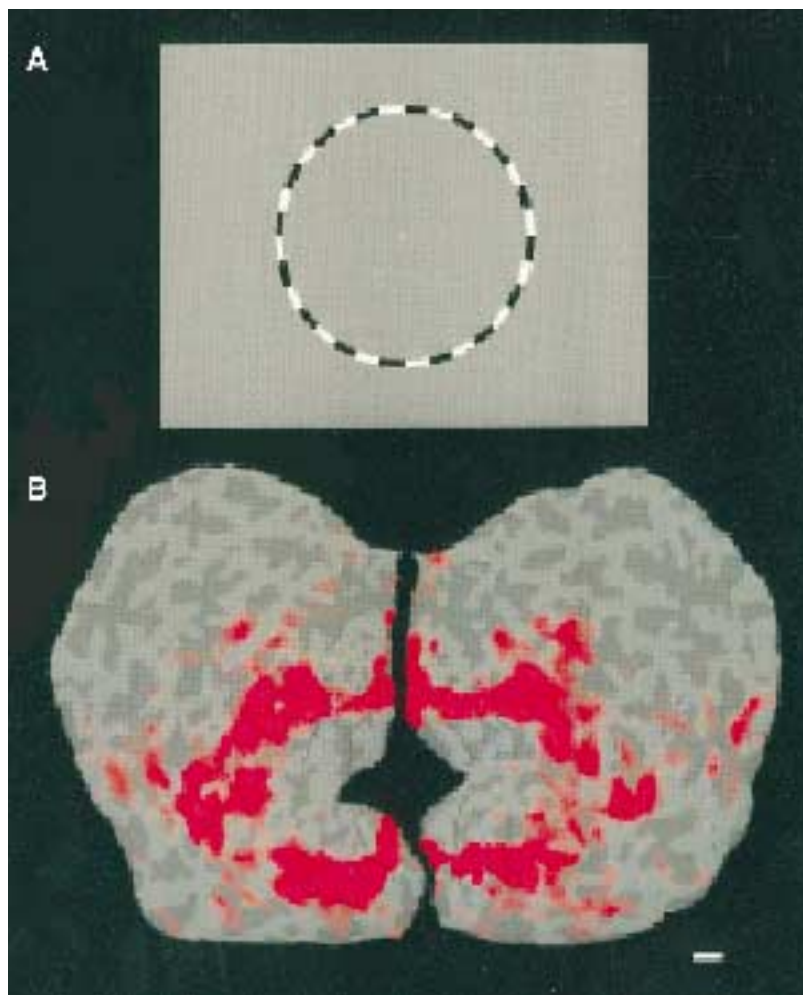
Fig. 3. *Apparent visual isomorphism in human cortical retinotopy.* **(A)** *The visual stimulus used to produce the activation shown in* **(B)**. *During functional magnetic resonance imaging (fMRI), the ring of checks remained stationary and the black-and-white checks within the ring reversed contrast (flickered) at 1Hz, while subjects fixated the central point. The image in* B *shows the flattened visual cortical surface from both hemispheres of one subject. The right hemisphere is on the right and the left hemisphere is on the left, consistent with a posterior viewpoint but reversed relative to radiological conventions. Medial brain locations appear towards the middle of the figure while lateral locations appear towards the left and right. Posterior locations appear near the middle of the figure and more anterior brain locations appear towards the midline and periphery. The semicircular ring is mapped on to roughly linearly shaped segments, orientated perpendicular to the long axis within each of the following human visual areas: V1; V2; V3; VP; V3A; and V4v. This result is consistent with predictions from the retinotopy and topography of the corresponding areas[39,40]. Very broadly, these areas form contiguous mirror-symmetrical wedges comprising a semicircular surface in each hemisphere. The borders between these areas were revealed by phase-encoded retinotopic mapping in the same subject (see, for example, Fig. 2C) and are also drawn on both hemispheres (vertical meridian representations are indicated by solid lines; horizontal meridian representations are indicated by dashed lines). Because of this arrangement, the composite activated line segments connect to form a rough semicircle in each hemisphere, so that the combined activation pattern from both hemispheres gives a complete 'circle'. Consistent with the increase in receptive-field size from areas V1 up to higher-order areas, the width and resolution of the composite activation 'circle' is thinnest in V1 and most diffuse in V3A and V4v. Scale bar, 1cm.*

information available from MT (V5). Perhaps the best-studied of these is MST, particularly the dorsal subdivision (MSTd). Several PET studies have suggested that certain foci activated in higher-order visual motion tests might correspond to a human MST area[24,62,64]; however, this has not been confirmed because of spatial and radiation limits. In some humans tested with fMRI, two different stimulus comparisons related to optic flow and the extent of ipsilateral visual-field activation convergently differentiate a single specific

portion of the area previously referred to as MT (V5), but not the remainder of that MT (V5) focus (see Fig. 2). Based on predictions from experiments in macaques, both of these stimulus comparisons should activate MSTd more than the (actual) MT (V5) area. Although more research is needed, this subregion (pMSTd in Fig. 2) is an excellent candidate for a human homolog of macaque MSTd.

One intriguing study[65] combined lesion and imaging data. In the akinetopsic (cortically motion-blind) patient described by Zihl *et al.*[18], PET techniques were used to measure brain activity produced during viewing moving and stationary visual stimuli. MT (V5) was not activated (presumably because of a lesion that included that area) but other motion-selective regions were revealed that might mediate the residual ability of this patient to perceive motion. In the future, this kind of functional imaging should greatly clarify psychophysical results obtained from patients with 'specific' cortical lesions.

Temporal stream

The first hint of a specialized temporal pathway for form and color recognition arose from studies in humans, not macaques. For more than a century, isolated reports have described damage to inferior occipital–temporal cortex that is accompanied by immediate and irreversible decreases in wavelength sensitivity (achromatopsia) in the affected hemifield, without impairment in other visual dimensions (like acuity and luminance contrast sensitivity) (reviewed in Ref. 68). Damage to nearby or overlapping regions can also lead to acute deficits in face recognition ('prosopagnosia') (reviewed in Ref. 69). Usually, symptoms of both achromatopsia and prosopagnosia are accompanied by upper visual-field loss but not always. Since the upper visual field is represented exclusively in retinotopic areas in inferior occipito–temporal cortical sites such as VP, ventral V2 and V4v, nonspecific damage to this region of the cortex would be expected to result in an upper-field loss[33,35–38].

Although several studies have proposed a possible location of human 'V4', the specific site of this area has proved difficult to resolve (see below). In macaques, 'V4' was originally defined as a large area immediately posterior to MT (V5). Subsequently, macaque V4 was extended ventrally along the entire anterior border of VP, so that V4 resembled area VA in owl monkeys (*Aotus*). That part of V4 nearest MT (V5) was eventually recognized as a separate area, known as V4A (Ref. 70) or V4t (Ref. 71).

Historically, macaque V4 has been the subject of controversy, not only with respect to its exact borders but also to its degree of color selectivity[72–75]. It should be emphasized that the ventral region of area V4 in macaques was never claimed to have high color selectivity, although ventral V4 is topographically most similar to the area damaged in human achromatopsia. However, increased color selectivity has been reported in areas near ventral V4 – in VP (Ref. 76) and inferotemporal cortex[77]. Recent studies in macaque V4 have focused on spatial-filtering properties in its receptive field, which are relevant for human imaging studies of form vision (Refs 78–80; see below).

Several neuroimaging studies[21,81,82] have reported color selectivity in an area of the human visual cortex that corresponds roughly to the area damaged in achromatopsia. Even if these results are confirmed in

other tests, it remains to be shown whether such a focus of color selectivity is co-extensive with a human 'V4', since the exact location of this area in humans remains ambiguous. fMRI mapping data have revealed a crudely retinotopic representation of the upper visual field immediately anterior to VP in human cortex, and this area was originally named 'V4v' (ventral V4)[33]. However, evidence for a corresponding lower visual-field representation (a human 'V4d') is weaker, which remains a puzzle.

A functionally defined region posterior to human MT (V5), called LO, is topographically similar to macaque V4 (Ref. 83). Like macaque V4 (including dorsal and ventral divisions), LO lies immediately posterior to MT (V5) and expands and curves posterio–inferiorly, anterior to VP. However, human V4v appears to be sandwiched neatly between LO and VP, in contrast to its location in current macaque maps (see Fig. 2).

Although macaque 'V4' has been difficult to recognize using architectonics, stains for lipofuscin in human cortex distinguish large pyramidal cells in a discrete region of the fusiform gyrus[84]. This magnocellular region overlaps the regions implicated in achromatopsia and prosopagnosia, area LO and some of the areas defined as ventral and dorsal 'V4'. It would be interesting to determine which functional region corresponds to this histologically distinct region.

Object recognition in the temporal stream

Studies of macaques suggest that visual information is processed in multiple stages, involving a gradual transformation of the retinal image from localized, spatially restricted representations in V1 to more global and complex representations in higher-order areas (reviewed in Ref. 80). Imaging experiments suggest a similar information-processing sequence in human visual cortex. There is a progressive decrease in retinotopic precision from primary visual cortex (including the posterior pole) to more lateral and anterior areas (for example, V3A and V4v), and it is lowest in visual areas lacking demonstrable retinotopy but showing good responses to visual stimuli (Refs 33,36; R.B.H. Tootell, A.M. Dale, J.D. Mendok Lui, J.B. Reppas and M.I. Sereno, unpublished observations). Conversely, antero–lateral areas lacking overt retinotopy can show striking global image selectivity (see below) to certain dimensions of visual motion or form. In information-processing streams of both motion and form, this conversion of initially retinotopic information might provide a basis for position- and scale-invariance at higher levels of the visual system.

In one fMRI study[83], site(s) of object-selective activation were localized relative to that of other visual areas. In most subjects, one general region ('LO') responded more to images of natural objects than to a wide variety of non-object control stimuli including textures, random dots, gratings, highly scrambled objects (several types of scrambling) and objects following Fourier phase randomization. The involvement of LO in object vision was also supported by its selective activation during the perceptual 'Lincoln' illusion (Ref. 85; see Fig. 5). However, activation in LO did not appear to be affected by object category or familiarity: familiar faces, common objects and unfamiliar abstract sculptures all activated LO to a similar degree. This combination of properties suggests that
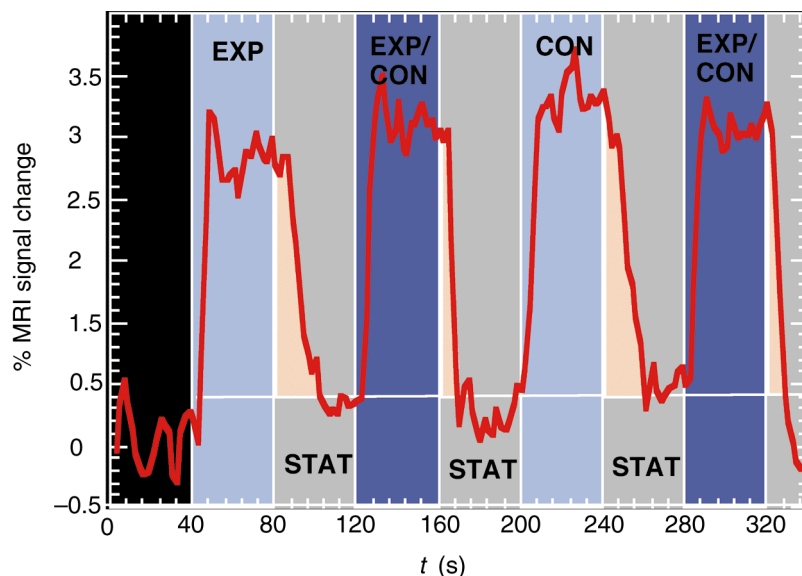

Fig. 4. *Averaged timecourse of functional magnetic resonance imaging (fMRI) signals in response to real and illusory motion from the middle temporal area (MT, or V5) of human visual cortex. Subjects were shown a pattern of concentric rings (50'' diameter) surrounding a fixation spot. In different periods (typically 40 s long) during each scan (5 min 40 s), the moving rings were continuously expanding (EXP), continuously contracting (CON) or reversing direction (expanding or contracting; EXP/CON) at 0.5 Hz. Within each local visual region, the direction of stimulus movement was either unidirectional (EXP and CON) or bi-directional (EXP/CON). Following every period of showing moving rings, stationary rings, otherwise equal (STAT), were presented. Following the periods of continuous unidirectional local motion (the expanding or contracting stimuli), a profound visual motion after-effect was seen in response to the (physically stationary) rings. Following the periods of reversing direction, no motion after-effect was reported. The response to stationary stimuli was only slightly greater than that to a blank field. This selective response to actually moving stimuli is consistent with other evidence from human and monkey MT (V5). The fMRI response amplitudes to both the single- and reversing-direction stimuli were essentially equal in amplitude. However, the fMRI response immediately following the single-direction stimuli (that is, when the illusory motion after-effect was visible) remained above steady-state response levels for approximately 25 s after stimulus offset, significantly longer than that predicted by the normal temporal response of the fMRI signal. On the other hand, fMRI responses following reversing-direction stimuli (when illusory motion after-effects were absent) returned more promptly to the steady-state response level produced by stationary stimuli. One interpretation of this result is that area MT (V5) remained activated because the stimulus appeared to be moving, even though it was physically stationary.*

LO acts as an intermediate processing stage interposed between primary visual cortex and higher-order, 'cognitive', object-recognition stages[83]. Similar results were obtained using PET techniques[86].

The fMRI signal in LO can be quite robust, even when generated by single images of objects. Such large signals presumably reflect the involvement of many neurons in each object representation, which would oppose the idea that objects are encoded by a very few, highly specialized 'cardinal' ('grandmother') neurons. Instead, it is likely that a broad population coding of either object 'prototypes' (see, for example, Ref. 87) or object components (see, for example, Ref. 88) underlies LO responses.

As in macaques, recent human imaging studies suggest that subsequent, more 'cognitive' stages involved in object identification activate more anterior and ventral areas. Electrical recording studies in humans[89] and recent PET (Ref. 90) and fMRI studies[91] all report selective activation in response to faces in locations ventral and anterior to LO. Two imaging studies[92,93] reported consistent deactivation by familiar (compared with novel) images in a 'stream' stretching from approximately LO along ventral temporal cortex to the hippocampus. An alternative organizational scheme
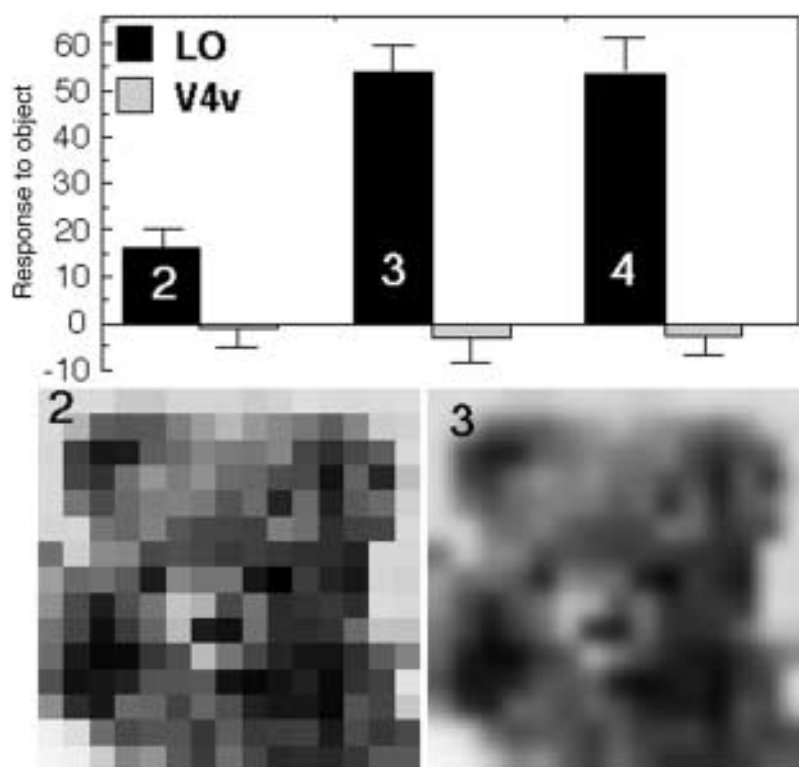
Fig. 5. The 'Lincoln' illusion. *The figure shows an averaged functional magnetic resonance imaging (fMRI) signal in area LO during the perceptual 'Lincoln' illusion. In this illusion, blocked images of objects have increased detectability when blurred. Subjects were shown: (1) a set of random blocks; (2) images of common objects and faces digitized into large blocks [example is shown in panel (2) at bottom left]; (3) same images as in (2) but blurred to increase detectability [example is shown in panel (3) at bottom right]; and (4) real-life images of the same objects. The bar histograms show the enhanced activation (%) during presentation of (2), (3) and (4) compared with activation in response to the random blocks (1, that is, zero on ordinate) in five subjects (average ± 1 SEM; n = 5) for LO (black) and the neighbouring area V4v (gray). Note that blurring the blocked images, which enhances object detectability, also produces enhanced activation in LO but not in neighbouring V4v (Ref. 83).*

for high-level object processing was suggested recently by a PET study in which detailed knowledge about object attributes was localized close to the cortical regions specializing in perceiving those attributes[94]. Undoubtedly, as more aspects of object recognition are mapped in the human cortex, and as the spatial resolution of the fMRI technique is improved, the sequence of transformations involved in object recognition will become clearer.

Human cortical connections

In experimental animals, borders of cortical areas have been defined convergently using four basic criteria listed by Van Essen and co-workers[31,39]: functional properties; retinotopy; histology; and connections. In human visual cortex, imaging studies have recently clarified the functional properties and retinotopy, and determined anatomists have described the human histology using autopsy material. The main gap in our knowledge of the human visual-cortex map concerns the cortical connections. Despite isolated reports[17,95,96], a technique does not yet exist that routinely and reliably maps intracortical connections in humans. Until specific cortical connections can be mapped directly, it will be impossible to construct an accurate hierarchy of visual cortical areas, as has been so crucial in cortical mapping of animal models.

One intriguing possibility is that anatomical connections could be inferred from cross-correlation functional imaging studies[97,98] but this has not yet been widely tested. Another possibility is to use fMRI or PET to constrain possible sources of activity from magnetoencephalogram or EEG signals (Refs 44,99; A.M. Dale, unpublished observations), thus extracting accurate latency information for known sources of activity and basing a connection hierarchy on this information. However, it will be difficult to infer a connectional hierarchy solely from such data because some pathways are more or less heavily myelinated than others, leading to slower or faster conduction times. Furthermore, differences exist in synaptic architecture at each neural stage, which likewise affect conduction time.

Selected references

1 **Gennari, F.** (1782) *De peculiari structura cerebri nonnullisque ejus morbis.* Parma, Ex regio typographeo
2 **Crick, F. and Jones, E.** (1993) *Nature* 361, 109–110
3 **Kaas, J.H.** (1993) in *Functional Organisation of the Human Visual Cortex* (Gulyas, B., Ottoson, D. and Roland, P.E., eds), pp. 1–12, Pergamon
4 **Sereno, M.I. and Allman, J.M.** (1991) in *The Neural Basis of Visual Function* (Leventhal, A.G., ed.), pp. 160–172, Macmillan
5 **Rosa, M.G.P. et al.** (1993) *Visual Neurosci.* 10, 827–855
6 **Payne, B.R.** (1993) *Cereb. Cortex* 3, 1–25
7 **Kaas, J.H.** (1995) *Curr. Biol.* 5, 1126–1128
8 **Braak, H.** (1976) *J. Comp. Neurol.* 166, 341–364
9 **Horton, J.C. and Hedley-Whyte, E.T.** (1984) *Philos. Trans. R. Soc. London Ser. B* 304, 255–272
10 **Tootell, R.B.H. and Taylor, J.B.** (1995) *Cereb. Cortex* 5, 39–55
11 **Wong-Riley, M.T.T.** (1993) in *Functional Organisation of the Human Visual Cortex* (Gulyas, B., Ottoson, D. and Roland, P.E., eds), pp. 165–180, Pergamon
12 **Hitchcock, P.F. and Hickey, T.L.** (1980) *Brain Res.* 182, 176–179
13 **Hendrickson, A.E. and Wilson, J.R.** (1979) *Brain Res.* 170, 353–358
14 **Tootell, R.B.H. et al.** (1983) *Science* 220, 737–739
15 **Hockfield, S., Tootell, R.B.H. and Zaremba, S.** (1990) *Proc. Natl. Acad. Sci. U. S. A.* 87, 3027–3031
16 **Horton, J.C. and Hoyt, W.F.** (1991) *Brain* 114, 1703–1718
17 **Clarke, S. and Miklossy, J.** (1990) *J. Comp. Neurol.* 298, 188–214
18 **Zihl, J., von Cramon, D. and Mai, N.** (1983) *Brain* 106, 313–340
19 **Fox, P.T. et al.** (1986) *Nature* 323, 806–809
20 **Fox, P.T. et al.** (1987) *J. Neurosci.* 7, 913–922
21 **Lueck, C.J. et al.** (1989) *Nature* 340, 386–389
22 **Zeki, S. et al.** (1991) *J. Neurosci.* 11, 641–649
23 **Watson, J.D. et al.** (1993) *Cereb. Cortex* 3, 79–94
24 **Corbetta, M. et al.** (1990) *Science* 248, 1556–1559
25 **Petersen, S.E. et al.** (1990) *Science* 249, 1041–1044
26 **Bandettini, P.A. et al.** (1992) *Magn. Reson. Med.* 25, 390–397
27 **Belliveau, J.W. et al.** (1991) *Science* 254, 716–719
28 **Kwong, K.K. et al.** (1992) *Proc. Natl. Acad. Sci. U. S. A.* 89, 5675–5679
29 **Ogawa, S. et al.** (1992) *Proc. Natl. Acad. Sci. U. S. A.* 89, 5951–5955
30 **Menon, R. et al.** *J. Neurophysiol.* (in press)
31 **Felleman, D.J. and Van Essen, D.C.** (1991) *Cereb. Cortex* 1, 1–47
32 **Engel, S.A. et al.** (1994) *Nature* 369, 525
33 **Sereno, M.I. et al.** (1995) *Science* 268, 889–893
34 **Van Essen, D.C. and Maunsell, J.H.R.** (1980) *J. Comp. Neurol.* 191, 255–281
35 **Schneider, W., Noll, D.C. and Cohen, J.D.** (1993) *Nature* 365, 150–153
36 **Tootell, R.B.H. et al.** (1995a) *J. Neurosci.* 15, 3215–3230
37 **Shipp, S. et al.** (1995) *Neuroimage* 2, 125–132
38 **DeYoe, E.A. et al.** (1996) *Proc. Natl. Acad. Sci. U. S. A.* 93, 2382–2386
39 **Van Essen, D.C. et al.** (1990) *Cold Spring Harbor Symp. Quant. Biol.* 5, 679–696
40 **Colby, C.L. and Duhamel, J.R.** (1991) *Neuropsychologia* 29, 517–537
41 **Olavarria, J. and Van Sluyters, R.C.** (1985) *J. Neurosci. Methods* 15, 191–202
42 **Tootell, R.B.H. and Silverman, M.S.** (1985) *J. Neurosci. Methods* 15, 177–190
43 **Drury, H.A. et al.** (1996) *J. Cogn. Neurosci.* 8, 1–28
44 **Dale, A.M. and Sereno, M.I.** (1993) *J. Cogn. Neurosci.* 5, 162–176
45 **Ungerleider, L.G. and Mishkin, M.** (1982) in *Analysis of Visual Behavior* (Ingle, D.J., Goodale, M.A. and Mansfield, R.J.W., eds),

pp. 549–586, MIT Press

46 Maunsell, J.H.R. (1987) in *Matters of Intelligence* (Vaina, L., ed.), pp. 59–87, Reidel

47 DeYoe, E.A. and Van Essen, D.C. (1988) *Trends Neurosci.* 11, 219–226

48 Livingstone, M. and Hubel, D.H. (1988) *Science* 240, 740–749

49 Zeki, S. and Shipp, S. (1988) *Nature* 335, 311–317

50 Goodale, M.A. and Milner, A.D. (1992) *Trends Neurosci.* 15, 20–25

51 Merigan, W.H. and Maunsell, J.H. (1993) *Annu. Rev. Neurosci.* 16, 369–402

52 Martin, K.A.C. (1988) *Trends Neurosci.* 11, 380–387

53 Haxby, J.V. *et al.* (1991) *Proc. Natl. Acad. Sci. U. S. A.* 88, 1621–1625

54 Gulyas, B. and Roland, P.E. (1994) *Eur. J. Neurosci.* 6, 1811–1828

55 Flechsig, P. (1920) *Anatomie des menschlichen Gehirns und Rückenmarks auf myelogenetischer Grundlage*, Thieme

56 Clark, S. (1994) *Eur. J. Neurosci.* 6, 725–736

57 DeYoe, E.A. *et al.* (1990) *Visual Neurosci.* 5, 67–81

58 Clark, V.P., Courchesne, E. and Grafe, M. (1992) *Cereb. Cortex* 2, 417–424

59 Dupont, P. *et al.* (1994) *J. Neurophysiol.* 72, 1420–1424

60 McCarthy, G. *et al.* (1995) *Hum. Brain Mapp.* 2, 234–243

61 Tootell, R.B.H. *et al.* (1995) *Nature* 375, 139–141

62 Zeki, S., Watson, J.D. and Frackowiak, R.S.J. (1993) *Proc. R. Soc. London Ser. B* 252, 215–222

63 Eden, G.F. *et al.* (1996) *Nature* 382, 66–69

64 De Jong, B. *et al.* (1994) *Brain* 117, 1039–1054

65 Shipp, S. *et al.* (1994) *Brain* 117, 1023–1038

66 Felleman, D.J. and Van Essen, D.C. (1987) *J. Neurophysiol.* 57, 889–920

67 Gaska, J.P., Jacobson, L.D. and Pollen, D.A. (1988) *Vision Res.* 28, 1179–1191

68 Zeki, S. (1990) *Brain* 113, 1721–1777

69 Damasio, A.R., Tranel, D. and Damasio, H. (1990) *Annu. Rev. Neurosci.* 13, 89–109

70 Zeki, S.M. (1983) *Proc. R. Soc. London Ser. B* 217, 449–470

71 Desimone, R. and Ungerleider, L.G. (1986) *J. Comp. Neurol.* 248, 164–189

72 Zeki, S.M. (1977) *Proc. R. Soc. London Ser. B* 197, 195–223

73 Schein, S.J. and Desimone, R. (1990) *J. Neurosci.* 10, 3369–3389

74 Heywood, C.A., Gadotti, A. and Cowey, A. (1992) *J. Neurosci.* 12, 4056–4065

75 Schiller, P.H. and Lee, K. (1991) *Science* 251, 1251–1253

76 Burkhalter, A. and Van Essen, D.C. (1986) *J. Neurosci.* 6, 2327–2351

77 Heywood, C.A., Gaffan, D. and Cowey, A. (1995) *Eur. J. Neurosci.* 7, 1064–1073

78 Desimone, R. and Schein, S.J. (1987) *J. Neurophysiol.* 57, 835–868

79 Gallant, J.L., Braun J. and Van Essen, D.C. (1993) *Science* 259, 100–103

80 Tanaka, K. (1993) *Science* 262, 685–688

81 Sakai, K. *et al.* (1995) *Proc. R. Soc. London Ser. B* 261, 89–98

82 Kleinschmidt, A. *et al.* (1996) *Exp. Brain Res.* 110, 279–288

83 Malach, R. *et al.* (1995) *Proc. Natl. Acad. Sci. U. S. A.* 92, 8135–8139

84 Braak, H. (1980) *Architectonics of the Human Telencephalic Cortex*, Springer-Verlag

85 Harmon, L.D. and Julesz, B. (1973) *Science* 180, 1194–1197

86 Kanwisher, N. *et al. J. Cogn. Neurosci.* (in press)

87 Edelman, S. (1995) *Minds Mach.* 5, 45–68

88 Fujita, I. *et al.* (1992) *Nature* 360, 343–346

89 Allison, T. *et al.* (1994) *Cereb. Cortex* 4, 544–554

90 Sargent, J., Ohta, S. and MacDonald, B. (1992) *Brain* 115, 15–36

91 Puce, A. *et al.* (1995) *J. Neurophysiol.* 74, 1192–1199

92 Vandenberghe, R. *et al.* (1995) *Neuroimage* 2, 306–313

93 Stern, C.E. *et al. Proc. Natl. Acad. Sci. U. S. A.* (in press)

94 Martin, A. *et al.* (1995) *Science* 270, 102–105

95 Burkhalter, A. and Bernardo, K.L. (1989) *Proc. Natl. Acad. Sci. U. S. A.* 86, 1071–1075

96 Kenan-Vaknin, G. *et al.* (1992) *Brain Res.* 594, 339–342

97 Friston, K.J. (1994) *Hum. Brain Mapp.* 2, 56–78

98 Biswal, B. *et al.* (1995) *Magn. Reson. Med.* 34, 537–541

99 Heinze, H.J. *et al.* (1994) *Nature* 372, 543–546

Dynamical representation of odors by oscillating and evolving neural assemblies

Gilles Laurent

Although smells are some of the most evocative and emotionally charged sensory inputs known to us, we still understand relatively little about olfactory processing and odor representation in the brain. This review summarizes physiological results obtained from an insect olfactory system and presents a functional scheme for odor coding that is compatible with data from other animals, including mammals. This coding scheme consists of three main and concurrent odor-induced phenomena: 20–30 Hz oscillatory mass activity; patterned and odor-specific neuronal responses; and transient, dynamic synchronization of odor-specific neural assemblies. When these phenomena are considered together, odors appear to be represented combinatorially by dynamical neural assemblies, defined partly by the transient but stimulus-specific synchronization of their neuronal components.

A REMARKABLE feature of olfactory systems is that their anatomical design (circuit macro- and microarchitecture, dendro–dendritic synaptic arrangements and neuronal morphologies) is exceptionally similar across animal phyla – from mollusks to insects, crustaceans and vertebrates[1–4]. Therefore, the functional principles that can be established from studying one system might apply to the others as well, because similar circuit design principles are likely (although by no means certain) to underlie similar functional or computational principles. In all cases but that of pheromonal olfaction, the problem to be solved by the brain is the specific representation of 'unpredictable' stimuli; that is, ones that, in the natural world, are complex and infinitely varied multicomponent blends[5]. Because odors are so varied, olfactory systems must be able to learn the specific patterns that make each smell what it is (for example, a rose or a

Gilles Laurent is at the California Institute of Technology, Biology Division, 139-74, Pasadena, CA 91125, USA.

PII: S0166-2236(96)10054-0   *TINS* Vol. 19, No. 11, 1996   **489**